Ligand-Mediated Targeting of Cytokine Interleukin-27 Enhances Its Bioactivity *In Vivo*

Marxa L. Figueiredo,[1,2] Manoel Figueiredo Neto,[1] Janelle Wes Salameh,[1,2] Richard E. Decker,[1] Rachel Letteri,[4] Delphine Chan-Seng,[3] and Todd Emrick[4]

[1]Department of Basic Medical Sciences, Purdue University, 625 Harrison Street, LYNN 2177, West Lafayette, IN 47907, USA; [2]Interdisciplinary Biomedical Sciences Program, West Lafayette, IN 47907, USA; [3]Universite de Strasbourg, CNRS, Institut Charles Sadron UPR22, F-67000 Strasbourg, France; [4]Department of Polymer Science & Engineering, University of Massachusetts, 120 Governors Drive, Amherst, MA 01003, USA

We have examined the role of a novel targeted cytokine, interleukin-27 (IL-27), modified at the C terminus with a dual targeting and therapeutic heptapeptide, in treating prostate cancer. IL-27 has shown promise in halting tumor growth and mediating tumor regression in several cancer models, including prostate cancer. We describe our findings on the effects of targeted IL-27 gene delivery on prostate cancer cells *in vitro* and *in vivo* and how the targeting enhances bioactivity of the IL-27 cytokine. We applied the IL-27 gene delivery protocol utilizing sonoporation (sonodelivery) with the goal of reducing prostate tumor growth in an immunocompetent TC2R C57/BL6 model. The reduction in tumor growth and effector cellular profiles implicate targeted IL-27 as more effective than an untargeted version of IL-27 in promoting bioactivity, as assessed by STAT1 and IFN-γ reporter genes. Moreover, enhanced antitumor effects and significantly higher accumulation of natural killer T (NKT) and CD8 effector cells in the tumors were observed. These results support a novel IL-27-based targeting strategy that is promising since it shows improved therapeutic efficacy while utilizing simple and effective sonodelivery methods.

INTRODUCTION

Our group and others have previously shown cytokine interleukin-27 (IL-27) to be a promising therapeutic for arthritis[1] and malignant tumors,[2–4] based on its multifunctional (immune stimulatory, antiangiogenic, pro-osteogenic) activity. For example, IL-27 helped prevent osteoclast formation and promote osteoblast differentiation,[2,3] key therapeutic features for treating bone-metastatic tumors. As such, *in vivo* gene delivery of IL-27 significantly reduced the rate of tumor growth and normalized bone density.[4] IL-27 is a heterodimeric cytokine composed of subunits IL27p28 (IL-27A) and EBI3 (IL27B) (Epstein-Barr virus-induced gene 3), which are related to the IL-12 subunits p35 and p40, respectively. IL-27 is immunomodulatory and was originally thought to be produced mainly by antigen-presenting cells in response to microbial or host immune stimuli. However, IL-27 recently has been shown to be involved in regulating immune response against tumor development and in serving as an "alarm" to sense inflammatory or infectious response to promote bone repair.[5] The receptor for IL-27, a heterodimer composed of

IL27Rα (WSX1) and IL6ST (gp130) subunits, is highly expressed in lymphoid organs, bone, normal, and tumor epithelial cells,[6,7] melanoma,[8] and leukemia.[9] IL-27 signaling induces TBX21 (T-bet), interferon-γ (IFN-γ), and IL-12-Rβ2 expression, promoting initiation of T helper 1 (Th1) differentiation.[10,11] Either systemic[12] or intratumoral[2] IL-27 treatments eliminate tumors without toxicity. IL-27 also shows antitumor activity through indirect mechanisms such as induction of natural killer and cytotoxic T lymphocyte responses or inhibition of angiogenesis through induction of CXCL9-10.[12]

Regarding IL-27 therapy delivery *in vivo*, we selected a method that utilizes clinically safe ultrasound (US) frequencies to induce cellular cavitation and deliver plasmid DNA via sonoporation (i.e., sonodelivery).[2] Previous studies using this method showed that the gene delivery efficiency can approximate that of adenovirus.[2] We have previously optimized sonodelivery conditions using reporter gene plasmids, finding that the best approach consisted of complexing plasmid DNA (pDNA) with a novel cationic polymer, termed rNLSd, in the presence of microbubble-assisted sonoporation.[13] In those studies, we observed that wild-type (WT) IL-27 sonodelivery slowed bone destruction and inhibited tumor growth.[4] However, one limitation of that approach was its moderate efficacy, in which tumor growth rate was reduced but tumors were not completely eradicated. Very recently, IL-27 delivery has employed creative methods including incorporating the cytokine within peptide-conjugated liposomes (ART1-IL-27) for controlling autoimmune arthritis.[14] These ART-1-IL-27 liposomes, when intravenously injected in arthritic rats, were more effective in suppressing disease progression than control-IL-27 liposomes lacking ART-1 or free IL-27 at an equivalent dose. ART-1-directed liposomal IL-27 offered a higher safety profile and an improved therapeutic index, supporting the concept that peptides can be used to direct proteins or nanoparticles for targeted delivery including biologics or small molecule compounds with enhanced efficacy and reduced systemic exposure. We hypothesized

that targeting the protein to tumor tissue by utilizing peptides that could bind receptors upregulated in tumor cells, such as the IL-6 receptor, could help augment IL-27 bioactivity.

For the purpose of targeting the IL-6 receptor, we selected a candidate heptapeptide from the literature, LSLITRL (S7 or "pepL"), which was first identified from a 7-mer random cyclic phage display screen targeting the IL-6 receptor alpha subunit (IL-6Rα).[15] This pepL inhibited IL-6 binding to IL-6Rα in a dose-dependent manner and could bind to the plasma membrane of IL-6Rα-expressing cell lines. The activity of pepL was attributed to its ability to antagonize IL-6 binding to IL-6Rα and inhibit phosphorylation of Akt and ERK1/2 mitogen-activated protein kinase (MAPK). This peptide reduced *in vivo* C33A human cervical carcinoma growth by ~75% and induced apoptotic cell death in tumors, establishing pepL both as a therapeutic and a targeting peptide.

We have also reported the strategy of a "model" for cytokine engineering that would promote targeting by using ~7–12 amino acid peptide ligands attached to the C terminus of a candidate protein via a short linker (GGGGS).[16] This C-terminal modification of secreted molecules enables their targeting and accumulation at tumor sites. We examined this concept with a secreted luciferase (Gaussia luciferase or Gluc) to mimic therapeutic protein secretion, targeting, and accumulation in tumors. Sonodelivery was employed with a biocompatible polymer complexed to pDNA to create a nanoplex, which was delivered along with microbubbles and sonicated to achieve ultrasound-enhanced muscle transfection.

There remains a lack of therapeutics that can simultaneously and effectively treat the prostate tumor while restoring affected bone tissue. Cytokine immunotherapies hold great promise because they are secreted molecules that can reach and treat both primary and distant secondary tumors. Thus, IL-27 targeting with a dual therapeutic and targeting C-terminal peptide, pepL, may augment cytokine bioactivity and efficacy against prostate tumors *in vivo*.

RESULTS

### Engineering of C-term Peptide Ligands Can Target Gluc to Tumor Cells

We designed a strategy to target cytokines to the IL-6Rα, a receptor increasingly reported to be upregulated in tumors of various types.[15] Because we sought to utilize targeting of cytokines to cells of both human and mouse origin, we generated a model for the mouse IL-6Rα and aligned it to the human IL-6Rα crystal structure model, as described in the Materials and Methods. The alignment suggested that the two receptors share high structural homology (Figure 1A). A peptide previously shown to bind IL-6Rα (pepL, LSLITRL) docks at regions with structural similarity in the receptor models for both species (Figure 1B). This pepL also has therapeutic activity since it has been reported to reduce signaling through this receptor.[15] We also generated a model with the human IL-6Rα (data not shown) to confirm that pepL is able to

interact with IL-6Rα at the interface between IL-6 and the IL-6Rα/gp130 receptor complex.

To model protein targeting and detect its binding to cells, we designed a Gluc molecule modified with the pepL peptide at its C terminus. We selected Gluc as an ideal "cytokine model" since this reporter protein has a signal peptide which enables its secretion from cells. As described in the Materials and Methods, Gluc plasmids were engineered to mediate expression of the protein with a linker and either a control non-specific sequence (Gluc.ns) or the peptide targeting IL-6Rα, pepL (Gluc.pepL). In order to best mimic *in vivo* applications of cytokine-based therapeutics, our rationale was to first produce culture-conditioned media (CCM) containing secreted Gluc. The Gluc molecules were expressed by C2C12 muscle cells transfected with a mammalian expression vector, and the CCM was collected for cell binding assays. We utilized firefly luciferase (luc) assays for STAT1 and STAT3 activity to compare the similarities or differences in signaling between the free peptides (ns pep or pepL) with Gluc.ns or Gluc.pepL, where the peptides are linked to the C terminus of the proteins. The effect of pepL appears to be relatively stronger as a free peptide in terms of STAT1 activation; however, the detrimental effect of activating the oncogenic STAT3 signaling also was observed (Figure 1C), where STAT3 was upregulated in two prostate cancer cell lines. In contrast, when the peptides are linked to the C terminus of a protein such as Gluc, the pepL only activated STAT1, whereas STAT3 was significantly downregulated by ~80% (p < 0.05) in three prostate cancer cell lines treated with Gluc.pepL as compared to Gluc.ns control (Figure 1C). The CCM was used in a binding assay with a variety of human and mouse cells (Figure 1D). Normal cells did not bind a significant amount of control (Gluc.ns) or targeted Gluc (Gluc.pepL), as assessed by a Gluc binding assay using CCM in Ad293, HEPG2, or normal prostate epithelial cells (NHPre1), whereas prostate tumor cells PC3, RM1, and TC2R showed up to ~10-fold increases in Gluc binding relative to Ad293 normal cells. Interestingly, differentiating bone cells (OB, MC3T3E1-14 or OC, RAW264.7) also showed a significant ability to bind Gluc.pepL (Figure 1D).

Sonoporation Delivery *In Vivo* Showed that Gluc.pepL Can Be Detected at Tumors

Our group utilizes sonoporation delivery (sonodelivery) to promote protein expression *in vivo*. Figure 2A depicts sonodelivery for expressing Gluc proteins in mouse muscle. An ultrasound (US) stimulus is applied to nanoplexes formed by plasmid DNA and cationic polymers (i.e., the "rNLSd polymers" with pendant VKRKKKP sequence) in the presence of microbubbles. Following delivery of nanoplex to skeletal muscle, the cytokine model protein (Gluc) is expressed *in vivo* with a C terminus peptide/ligand tag (pepL) (Figure 2A). Gluc is expressed in the hind thigh muscle (dorsally), while the tumor cells are located ventrally, following intratibial implantation (proximal to the knee). *Ex vivo* evaluation at day 10–14 via sensitive bioluminescence imaging (BLI) showed that signals of targeted G.uc.pepL (but not the control G.uc.ns) were significantly enhanced only in the targeted area (i.e., at the tumor:bone interface), but not
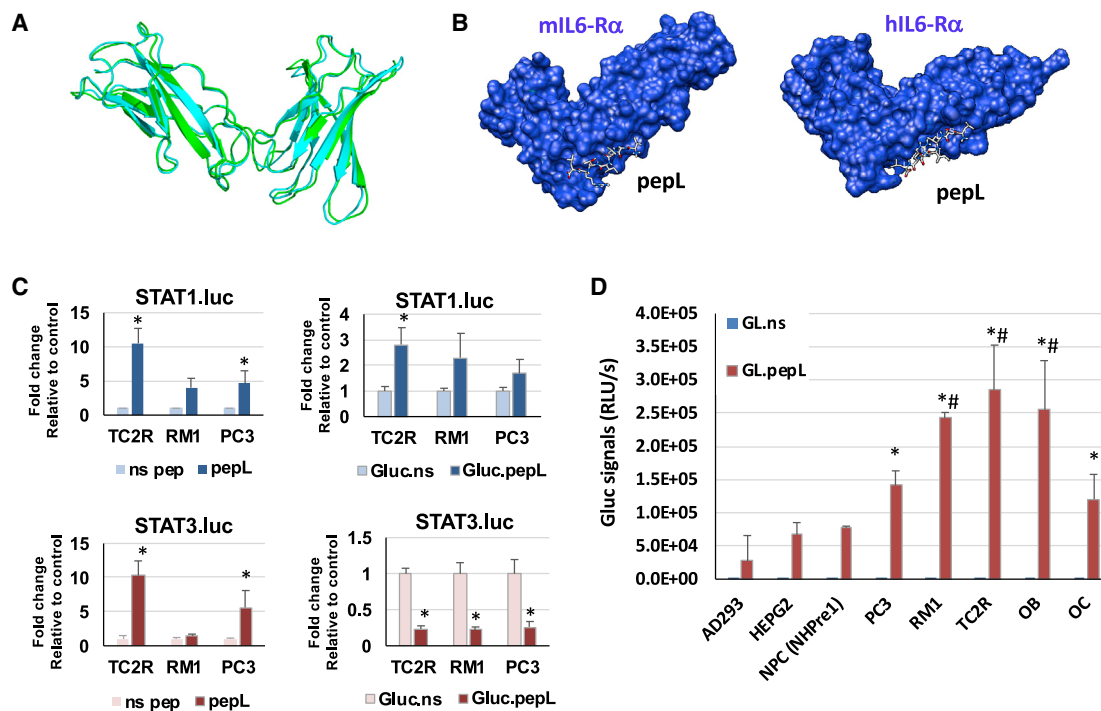
Figure 1. C-term "Peptide L" (pepL) Can Target an Engineered Cytokine Model Protein (Gaussia Luciferase) to Tumor Cells.

(A) Alignment of mouse and human IL-6Rα illustrates the degree of structural homology between these two species. (B) A model of pepL interactions with the mouse or human IL-6Rα, as detailed in Materials and Methods. (C) STAT1- or STAT3-luc reporter assays show upregulation of STAT1 but also upregulation of STAT3 by the free pepL (a peptide targeting the IL6-Rα) relative to a non-specific control free peptide (ns pep). The engineering of the pepL or non-specific control to an irrelevant protein (Gaussia luciferase or Gluc) enabled pepL to activate STAT1 but not STAT3, relative to ns pep control. Cells were transfected with STAT3-luc reporter vector and treated with conditioned media (generated in C2C12 cells) containing either control or peptide-modified Gluc, as described in Materials and Methods. *$p < 0.05$ relative to control (ns pep or Gluc.ns) levels of STAT1- or STAT3-luc activity. (D) An *in vitro* assay for detecting Gluc binding to cells. Gluc engineered at the C-term (Gluc.ns or pepL) were expressed from a mammalian expression vector in C2C12 muscle cells. The culture conditioned media (CCM) was collected and used in a binding assay using normal cells (AD293, HEPG2, or NHPre1), tumor cells (PC3, RM1, TC2R), or differentiating bone cells (OB, MC3T3E1-14 preosteoblasts and OC, RAW264.7 at day 4). *$p < 0.05$ compared to Gluc.ns CCM. Data is expressed as mean +- the standard deviation.

in normal organs of mice bearing TC2R tumors intratibially (Figure 2B; color bar, p/sec/cm²/sr). Normal organs evaluated included the liver, lung, heart, small intestine, kidney, pancreas, and spleen. Remarkably, there was a ~13-fold increase in Gluc.pepL accumulation in tumor samples, which was significant ($p < 0.012$) relative to untargeted Gluc-treated animals in *ex vivo* quantification of tumor tissue signals (Figure 2B, right plot).

We proceeded to modify the C terminus of a cytokine that we previously identified as a promising therapeutic agent for both tumor and bone, IL-27,[3,4] in the same manner described for Gluc. T The mouse EBI3-IL-27p28 "hyper IL-27" as a fusion protein of the heterodimer components, since it is more potent than delivering each single monomer.[17] This IL-27 was then engineered at its C terminus with a GGGGS linker and peptide ligands pepL or non-specific control (ns) as described in Materials and Methods to generate IL-27.pepL or IL-27.ns. These C-termini-modified IL-27 vectors were tested *in vitro* for their ability to express IL-27 (data not shown) and for stimulating IL-27 downstream signaling, as assessed by reporter gene constructs such as STAT1-luc. We reasoned that since free

pepL displayed oncogenic STAT3 activation in the reporter assay (Figure 1C), we could proceed solely utilizing the C terminus linked pepL design, which significantly activated STAT1 while significantly downregulating STAT3 in three prostate cancer cell lines (Figure 1C). We examined the bioactivity of these C-term-modified IL-27 proteins *in vivo* as described in the following section.

In Vivo Bioactivity of Targeted IL-27.pepL Is Enhanced Relative to Untargeted IL-27.ns

Following generation and examination of a model depicting that pepL would be accessible on the surface of IL-27 (Figure 3A), we designed an *in vivo* bioactivity assay whereby implanted "sensor" cells could express the reporter gene luciferase in response to IL-27. This assay would enable real-time *in vivo* detection of IL-27 activity. First, animals received plasmids pMCS ('multiple cloning site' or empty vector, pcDNA3.1), pIL-27.ns, or pIL-27.pepL intramuscularly via sonodelivery to promote cytokine expression (IL-27.ns or IL-27.pepL) for 3 days. The hind thigh muscle received 12.5 μg of plasmids complexed with polymer rNLSd and microbubbles in the presence of an ultrasound stimulus. 3 days after sonodelivery, "sensor" cells (TC2R
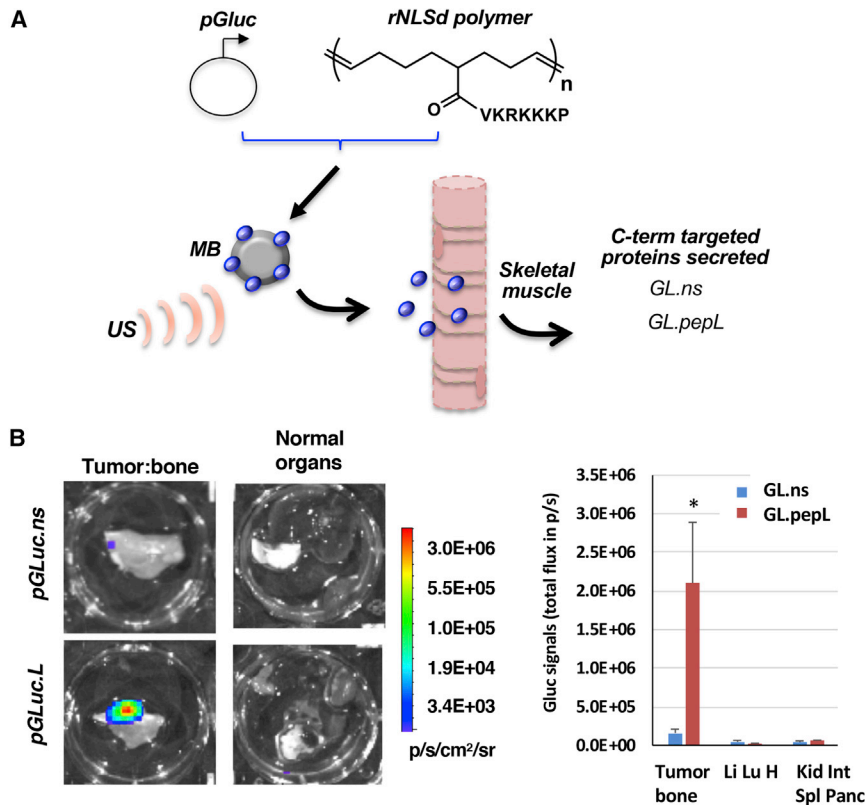
Figure 2. Sonodelivery of Gluc Fusion Proteins *In Vivo*

(A) Schematic of sonodelivery for expressing Gaussia luciferase (Gluc) proteins in mouse muscle. Nan Nanoplex formation with the rNLSd polumer was performed as described in Takeda et al.,[11] complexed with plasmid DNA encoding Gluc. NN This nanoplex is delivered in the presence of microbubbles (MB) as described in Materials and Methods. An ultrasound stimulus (US) is applied to disrupt the MB and the nanoplex of polymer:pGluc mediates skeletal muscle cell transfection. The proteins secreted contain a C-terminal peptide tag that either targets the IL-6Rα (pepL) or is untargeted (non-specific peptide control). (B) *Ex vivo* Gluc imaging post-gene delivery. Bioluminescence imaging is shown using coelenterazine substrate on organs isolated from animals receiving control (Gluc.ns) or ligand targeted Gluc (Gluc.pepL). Color bar, p/sec/cm^2/sr. Signals are present in the tumor:bone region only when targeted Gluc.pepL is delivered to muscle. Right plot, average Gluc signals from tumor:bone *ex vivo* pooled from day 10 and 14 post-delivery (*$p < 0.013$ for comparing Gluc.pepL relative to Gluc.ns accumulation in tumor tissue (accumulation in normal organs not significantly different between Gluc.ns and Gluc.pepL). Normal organs included an imaged pool of either liver, lung and heart (Li, Lu, H) or kidney, small intestine, spleen, and pancreas (Kid, Int, Spl, Panc). Mice were bearing TC2R tumors intratibially. Data is expressed as mean +- the standard error of the mean.

cells transfected with either STAT1 or IFN-γ-responsive luc vectors) were implanted in the flanks of the animals. TC2R prostate cancer cells were chosen because they exhibit IL-6-Rα upregulation. Luciferin substrate was administered intra-peritoneally 24 h later and signals were detected as a surrogate for IL-27 bioactivity (Figure 3B). STAT1- or IFN-γ-luciferase signals were detectable only in animals that received IL-27.ns or IL-27.pepL (Figure 3B). Quantification of the bioluminescence signals showed that animals treated with pIL-27.ns had a 2-fold increase of luc activity at the cell implantation sites compared to the control vector (pMCS) (Figure 3C). The animals receiving pIL-27.pepL also had a significant increase in luc signals relative to both control pMCS (*$p < 0.05$) and pIL-27.ns (#$p < 0.05$) (Figure 3C). This correlates to a higher bioactivity with the IL-27.pepL C-term fusion.

The IL-27 Targeting Mechanism Appears to Involve Both Paracrine and Autocrine Signaling

We next wanted to examine the potential modes of signaling for the C-term-modified IL-27. We suggest a model by which the peptide allows anchoring of cytokines to cells expressing targeting receptors (for example, IL-6Rα) (Figure 4A). This model proposes that the IL-27 in the CCM could signal in different cells in both autocrine and paracrine modes (Figure 4). We designed an experiment to examine this model, whereby we confirmed that C-term pepL modification enhances IL-27 signaling *in vitro*. In the autocrine

design, pSTAT1-luc and pIL-27 vectors were co-transfected (Figure 4A).

In the paracrine design, either differentiating osteoblast (OB, MC3T3E1-14, day 4) or epithelial cells (TC2R) were transfected with STAT1-luc, then mixed with the other cell type expressing either IL-27.ns, IL-27.pepL, or empty vector control (pMCS). In order to have an effect, IL-27.pepL had to be secreted from one cell type and bind to the other cell type (bearing STAT1-luc) to induce signaling (Figure 4B). In both designs, the C-terminal pepL enhanced IL-27 signaling ($p < 0.04$ versus ctrl, #$p < 0.05$ versus IL-27) up to 4.4-fold (autocrine design) and up to 3-fold (paracrine design) relative to pMCS or basal co-culture controls. The IL-27.pepL-mediated increases in paracrine signaling could be blocked by addition of a specific anti-IL-6Rα antibody (Figure 4B).

IL-27 Targeting with pepL Modifies Gene Expression in Tumor Cells

To better understand the potential mechanisms underlying the differences in bioactivity between IL-27.pepL and IL-27.ns, we examined genes up- or downregulated by IL-27.ns and IL-27.pepL relative to control vector (MCS) in transfected TC2R cells. As expected, the IL-27.ns vector promoted ~20-fold upregulation of transgene expression, as assessed by qPCR using primers specific for IL-27p28 and EBI3 subunits (Figure 5A; $p < 0.05$ relative to control MCS). Interestingly, we observed further upregulation of transgene
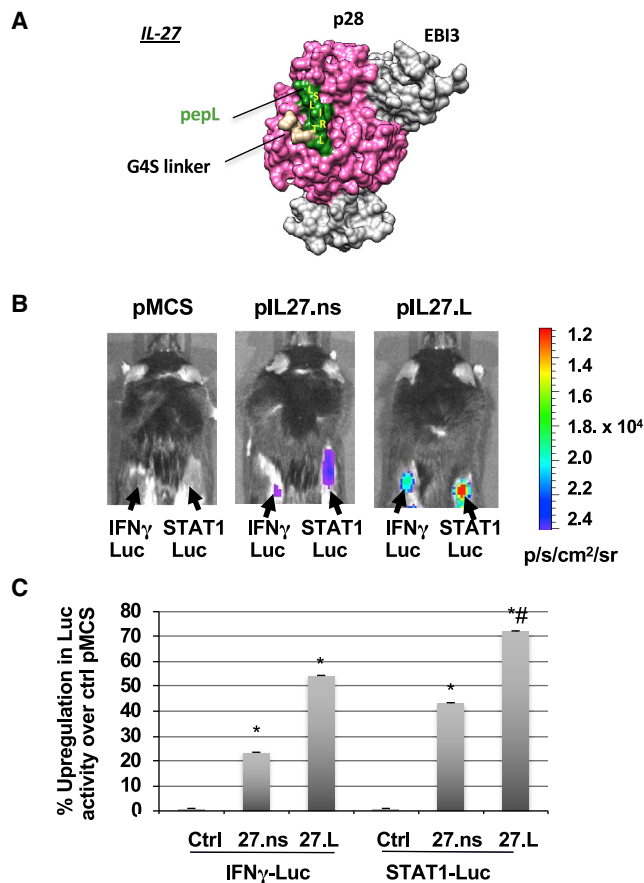
Figure 3. Ligand-Targeted IL-27 Has Enhanced Bioactivity *In Vivo*, Stimulating STAT1 and IFN-γ Signaling in Target Cells

(A) A model of IL-27.pepL showing IL-27p28 and EBI3 subunits, the G4S linker, and the pepL peptide. (B) The bioactivity of IL-27.pepL *in vivo* using TC2R prostate cancer cells. Cells were transfected with luciferase reporter vectors containing either STAT1 binding sites or the IFN-γ promoter to generate "reporter cells." Equal numbers of reporter cells (7.7×10^5) were implanted in the flanks of C57BL6 males (n = 6) that had received in the hind thigh 3 days prior by sonoporation 12.5 μg of plasmid DNA (either empty control pMCS, IL-27 with a non-specific peptide [ns] at the C terminus, or C-term-targeted IL-27 (IL-2.7pepL). pDNA were delivered via sonodelivery (polymer NLSd+ultrasound+MB). 24 h post-cell injection (i.e., day 4 post-sonoporation of pDNA), the effect of IL-27.ns or IL-27.pepL can be visualized in the presence of luciferin substrate. Bioluminescent signals were detectable using an IVIS100 Xenogen imager only in animals that received pIL-27.ns or pIL-27.pepL but not pMCS control vector. Color bar, $p/sec/cm^2/sr$. (C) Fold increase of luciferase activity of pIL-27.ns or pIL-27.pepL compared to pMCS-treated. Animals treated with pIL-27.ns had an increase of luc activity compared to pMCS control vector (*p < 0.04). The animals receiving pIL-27.pepL had a further increase in luc activity relative to the pIL-27.ns treated sites (#p < 0.03). Data is expressed as mean +- standard deviation.

expression when IL-27.pepL was delivered, toward a ~60- to 80-fold upregulation of IL-27p28 and EBI3 relative to IL-27.ns (Figure 5A; #p < 0.05). The observed upregulation of IL-6 prompted us to query the expression of several target genes associated with IL-6 or IL-27 responses as described in Hirahara et al.[18] The IL-27.pepL effect differed from the IL-27.ns control primarily by promoting significant

upregulation of SOCS3 and XCL1 (Figure 5B). Gene expression of several cytokines relevant to the tumor microenvironment also were assessed, and both IL-27 constructs promoted significant upregulation of IL-6, IL-18, and CXCL10 to ~2- to 3-fold (Figure 5C; *p < 0.05). However, the IL-27.pepL construct promoted further upregulation of IL-6, IL-18, and CXCL10, as well as upregulation of TNF and IL-1β relative to IL-27.ns (Figure 5C; #p < 0.05). Based on previous studies where IL-27 modulated infiltration of lymphocytes to tumors,[2,4] we also examined key immunogenic genes.[19] Although all immunogenic genes were significantly upregulated by the IL-27.ns relative to control MCS, IL-27.pepL delivery significantly augmented the upregulation by an additional ~2- to 3.5-fold (Figure 5D). These types of gene expression changes also were confirmed in tumors using qPCR, where we detected significant upregulation of IL-27p28, EBI3, TBX21, XCL1, and IFN-γ by ~2.7- to 4.9-fold in tumors treated with IL-27.pepL relative to IL-27.ns (data not shown).

Ingenuity pathway analyses (IPA) included (1) comparison analyses between TC2R cells treated with IL-27.ns versus IL-27.pepL, both corrected for control pMCS qPCR expression levels and (2) individual core analyses of each treatment group versus pMCS. Canonical pathway analyses representations yielded a heatmap with ranked activation Z scores (-2.0 to $+2.5$) (Figure 6A) and cellular and organismal functions also ranked in a heatmap by the $-\log$ Benjamini-Hochberg (B-H) of p values (Figure 6B), as described in Materials and Methods, and upstream regulators[20] (Table 1). Upstream regulator analysis indicated that, relative to control pMCS, the IL-27.ns-treated TC2R cells had IPA-predicted upstream or causal regulators that included IL-12, LPS-like effect, IFN-γ, and Toll-like receptor 4 (TLR4; p < 0.01). Top regulator effect networks included primarily activation of IL-18, but also FOXO1, IRF4, and IFN-γ and inhibition of MYC, collectively relating to the function *accumulation of leucocytes*. The IL-27pepL-treated TC2R had some of the same IPA-predicted upstream or causal regulators, including IL-12, and TLR4, but some different predicted regulators including IL-27RA, IL-10, and NOD2, relating to the functions *lymphoid tissue structure and development* and *immune cell trafficking*. Cellular and organismal functions included *communication between immune cells*, *altered immune cell signaling*, *IL-10 signaling*, and several other immune-related functions.

IL-27 Targeting Enhances Antitumor Activity and Effector Cell Recruitment to Prostate Tumors

Next we examined the effects of IL-27.pepL expression relative to IL-27.ns or control (pMCS) vector delivery *in vivo*. TC2R cells were implanted in C57/BL6 male mice subcutaneously; tumor growth was monitored by caliper measurements. Plasmids (12.5 μg) were delivered to the hind thigh intramuscularly at day 4 using sonoporation. IL-27.pepL proved more effective at halting tumor growth than IL-27.ns or empty vector control (pMCS) (Figure 7A; *p < 0.05 relative to pMCS control; #p < 0.05 relative to IL-27.ns). Tumor growth inhibition was calculated between days 3 and 18, and growth rate was inhibited by 50% for pIL-27.ns and by 89% for pIL-27.pepL-treated tumors relative to control pMCS-treated tumors. Serum levels of IL-27,
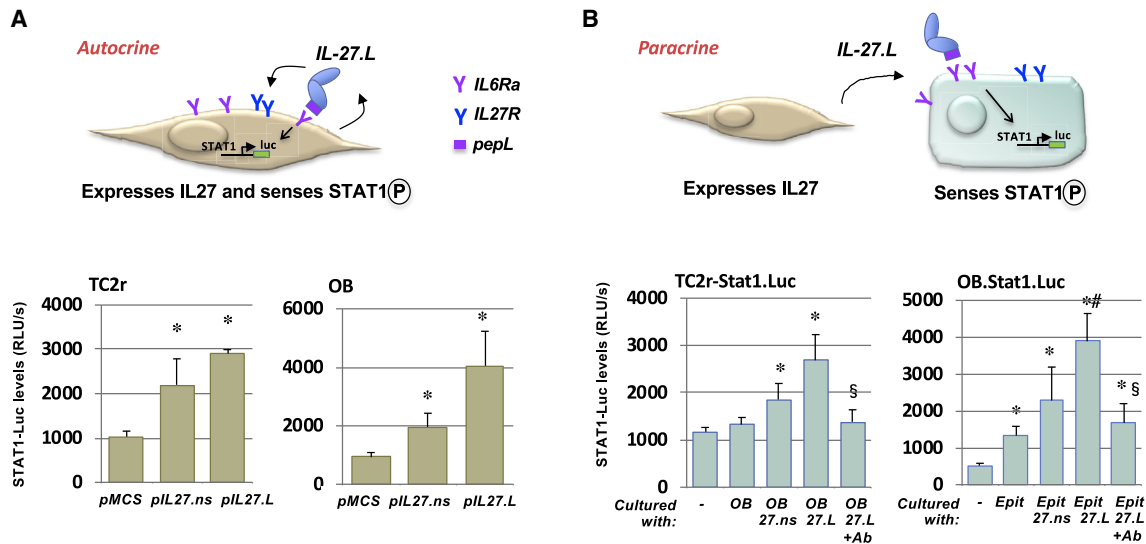
Figure 4. Targeted IL-27 Utilizes Both Paracrine and Autocrine Signaling

(A) pepL-modified IL-27 utilizes autocrine mode of signaling. In the autocrine design, the plasmids expressing IL-27 were delivered along with a reporter plasmid (STAT1-luc). The IL-27 C-term pepL (IL-27.pepL) allows anchoring of cytokine to the overexpressed targeting receptors (IL-6Rα). The cytokine is expressed and acts on the IL-27R to mediate STAT1 signaling. (B) PepL enhances IL-27 signaling also in a paracrine mode. In the paracrine design, either differentiating osteoblast (OB, MC3T3E1-14 day 4) or epithelial cells (TC2r) were transfected with STAT1-luc, and then mixed with the other cell type expressing IL-27.ns, IL-27.pepL, or empty vector control. In order to have an effect, IL-27.pepL had to be secreted from one cell type and bind to the other cell type (bearing STAT1-luc) to induce signaling. In the autocrine design, pSTAT1-luc and pIL-27s were cotransfected. The paracrine signaling effect can be blocked by pretreatment (30 min) with an anti-IL-6Rα blocking antibody (Ab). *p < 0.04 versus control, #p < 0.05 versus IL-27.ns. *p < 0.05 versus ctrl MCS or no cell coculture (comix); #p < 0.05 versus 27.ns; $p < 0.05 AB 27L versus 27L. Data is expressed as mean +- the standard deviation.

detected using ELISA for IL-27p28, showed levels that peaked early on and decreased throughout the study for both IL-27.ns and IL-27.pepL (Figure 7B). Both IL-27-treated groups had significantly higher IL-27 serum levels relative to pMCS control (Figure 7B) in general, but these increases were only significant for early- and mid-time points. The IL-27.pepL had significantly higher IL-27p28 serum levels at the early time point relative to IL-27.ns.

Finally, we examined whether therapy modified the extent of tumor-infiltrating lymphocyte populations. We observed a significant upregulation in γδT and NKT for both IL-27 therapies (Figure 7C; *p < 0.05). However, the IL-27.pepL displayed some differences from IL-27.ns control, including a higher level of CD3/8 and NKT cells (#p < 0.05 relative to IL-27.ns), reductions in CD19 cells, and normalization of CD4/25 and NK toward control pMCS-treated levels (p < 0.05).

DISCUSSION

In this work, we addressed the fusing of C-terminal peptide ligands to Gluc, a cytokine model protein, and to IL-27, a therapeutic cytokine. We selected a peptide reported to have targeting ability toward the IL-6Rα. Our results suggest that this peptide could be useful to target and treat aggressive prostate tumors, since the receptor and the STAT3 signaling axes are upregulated in ~95% of human prostate cancer tumor metastases relative to normal tissues.[21] We also observed that this receptor might be used for targeting differentiating

osteoblasts and osteoclasts, which is supported by reports of upregulated IL-6Rα levels in vivo as osteoblasts[22] and osteoclasts[23] differentiate. The heptapeptide LSLITRL (pepL) was modeled onto the available crystal structure of the hIL6-Rα/gp130 complex, suggesting that the pepL would disrupt signaling through this receptor pair. Also, the mouse/human receptor model alignments, along with our in vitro and in vivo data, indicate that pepL is functional in mouse cells. Signaling through IL-6Rα appeared to be inhibited by the Gluc.pepL fusion but not by free pepL as assessed by STAT3 activity measured using a luc reporter vector. Also, the effect of pepL appeared to be stronger as a free peptide in terms of STAT1 activation; however, activation of the oncogenic STAT3 signaling also observed suggest that utilizing the free pepL could be detrimental to therapy strategies. This result indicated that the pepL, if provided in the right context (linked at the C-termini), can have a dual targeting and therapeutic function for prostate cancer applications, as has been suggested to have for other tumors.[15] Gluc.pepL also could preferentially accumulate at the tumor/bone interface in vivo rather than in normal tissues, implicating this peptide in targeting a cytokine model protein (Gluc) to specific locations. The Gluc fusion with pepL (Gluc.pepL) showed a ~10- to 13-fold increase in binding to tumor cells relative to normal control cells.

Engineering at the C-terminus of the therapeutic cytokine of interest, IL-27, with pepL resulted in higher bioactivity in vivo relative to a non-specific control peptide, as assessed by IFN-γ and STAT1 signal
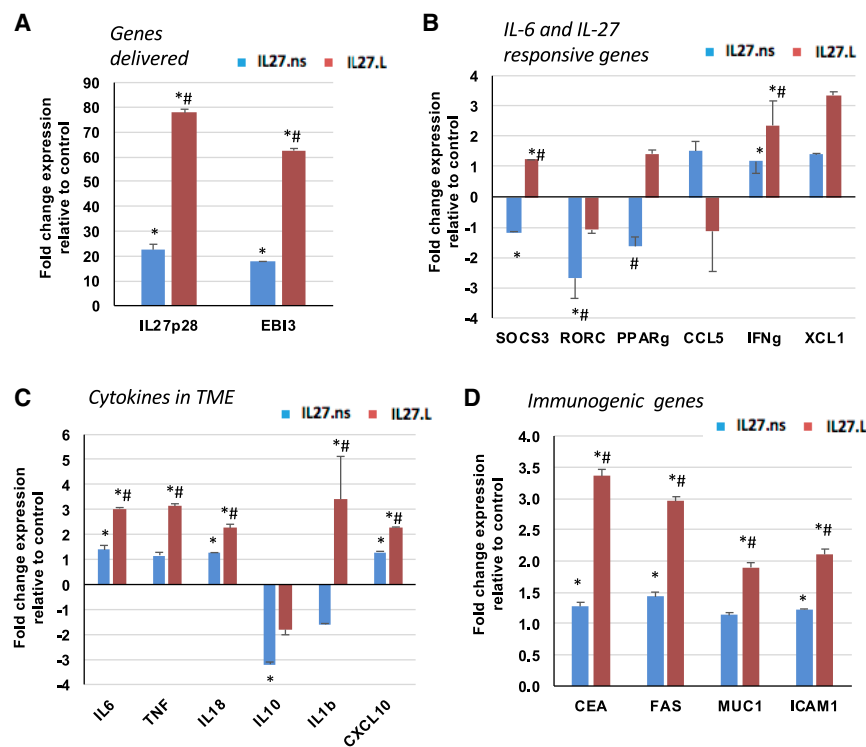
Figure 5. Differential Gene Expression by qPCR Analysis following Gene Delivery in TC2R

Following gene delivery of TC2R cells with either control (pMCS), pIL-27.ns, or pIL-27.pepL, and qPCR analysis, the cells transfected with pIL-27.ns or pIL-27.pepL had different patterns of up-(red) and downregulation (blue) of gene expression relative to control. Fold changes in expression relative to control pMCS are shown at 24 h-post transfection in (A) genes delivered (IL-27p28 and EBI3), (B) IL-6 and IL-27 responsive or target genes, (C) genes representing cytokines in the tumor microenvironment, and (D) immunogenic genes. *p < 0.05 relative to control pMCS transfected cells; #p < 0.05 relative to pIL-27.ns transfected cells. Data is expressed as mean +- the standard deviation.

detection in responsive cells. This higher bioactivity led us to examine whether the targeting mechanism might involve paracrine and/or autocrine signaling mechanisms. *In vitro* experiments suggested that the mode of signaling for the IL-27.pepL can involve both autocrine and paracrine mechanisms, i.e., it can have effects on the same or neighboring cells and promote STAT1 signaling as assessed by luc reporters. This is important for gene delivery since IL-27 can impact both the targeted cell (tumor), as well as neighboring cells (bone cells or other tumor cells, for example). The experiment shown in Figure 4 suggests that the chimeric IL-27.pepL molecule still can signal through its own receptors since blocking the IL-6Rα with a specific antibody reduced the STAT1 signaling, but only to a level equivalent to that of wild-type IL-27. The C-term modified cytokine thus has a dual function (pro-IL-27 and anti-IL-6 signaling) and constitutes a novel therapeutic cytokine. Overall, the pepL appears to enhance the antitumor activity of IL-27 *in vivo*, augmenting the protective immune responses that IL-27 already can mount against exogenous and endogenous tumors,[24] which is critical as the basis for future development of an IL-27-based therapeutic agent. The enhanced STAT1 and IFN-γ expression utilized *in vivo* as a surrogate for IL-27's bioactivity were particularly important to validate that a C-term modification (pepL) that enhanced targeting did not disrupt IL-27's ability to signal through these pathways. Combined with the targeting visualized with Gluc.pepL as compared with Gluc.ns, the data suggests that the pepL is able to target cytokines to tumors. When combined with a cytokine such as IL-27, the effect appears to be magnified, enabling further enhancements in IL-27 bioactivity and/or signaling.

Gene expression analyses by qPCR and IPA analyses indicated that the therapeutic cytokines differed in many respects. Interestingly, gene expression results following delivery of control or IL-27 vectors indicated that IL-27.pepL potentially has a stronger effect in cells and *in vivo*. This effect could be attributed to an ability to promote a positive feedback upregulation of IL-27 and regulated genes. Also, IL-27.pepL enhances expression of several immunogenic genes and differentially modulates expression of several cytokines that can significantly alter signaling in the tumor microenvironment. Upregulation of TNF, IL-18, IL-1β, and CXCL10 can alter the profile of immune effectors recruited to participate in the immune response against tumors. In particular, CXCL10 has been reported as a chemotactin for NKT and CD8 cells,[25] and this may underlie the augmented NKT and CD8 infiltration we detected in TC2R tumors. Interestingly, IL-27.pepL also upregulated IL-6, perhaps as a compensatory mechanism for the pepL-mediated signaling inhibition. When either IL-6 or IL-27 responsive genes were examined,[18] it became apparent that IL-27.ns downregulated the three IL-6 responsive genes and upregulated as a trend all three IL-27 responsive genes (although some not significantly). In contrast, IL-27.pepL significantly upregulated IL-6 responsive gene SOCS3 and as a trend, PPARγ. This activity is likely due to the IL-6 gene expression activation. IL-27.pepL significantly upregulated IFN-γ and XCL1 (another strong lymphocyte chemotactin), suggesting that the pepL can magnify some while opposing other IL-27 signals. Further development of this IL-27.pepL or similarly targeted therapies would aim to reduce IL-6 upregulation and further enhance IL-27 signaling for an augmented therapeutic effect. These types of gene expression changes were confirmed in tumors, where we detected upregulation of IL27p28, EBI3, TBX21, XCL1, and IFN-γ when tumors had been treated with IL-27.pepL relative to IL-27.ns.

Individual IPA analyses of each IL-27 dataset relative to pMCS indicated that several canonical pathways were impacted differently by IL-27.pepL relative to IL-27.ns. The upstream regulators analysis
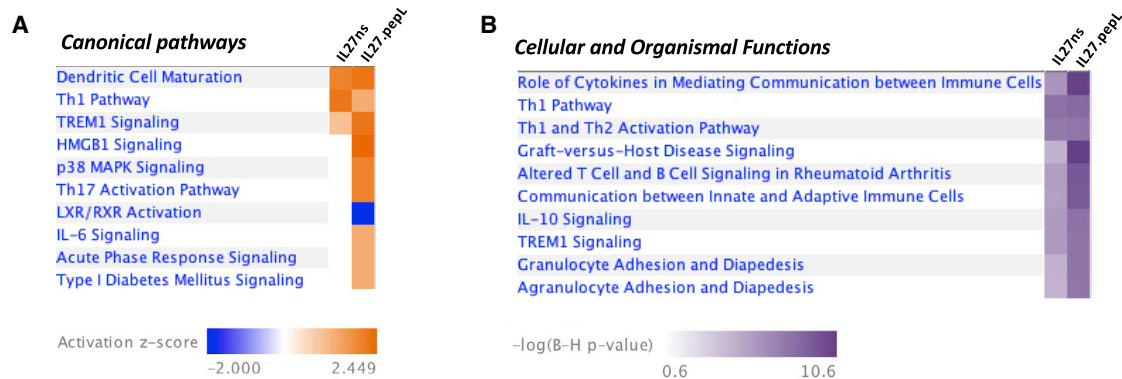
Figure 6. Heatmap of Canonical Pathways Predicted by IPA to Be Altered between Cells Expressing IL-27.ns and IL-27.pepL

A comparison analysis was performed between samples of TC2R cells transfected with plasmid expressing IL-27.ns and IL-27.pepL (both corrected to pMCS vector control) as per the IPA analyses described in Materials and Methods. (A) Canonical pathways that differ between the IL-27.ns and IL-27.pepL treatments. Color bar, activation *Z* scores. (B) Cellular and organismal functions that differ between the IL-27.ns and IL-27.pepL treatments. Color bar, −log(B-H p value).

indicated several potential upstream regulator differences between treatments, and these would be excellent for providing candidates for co-expression to augment efficacy or effect of IL-27.pepL therapy in future studies. IPA analyses implicated other networks that can be utilized with IL-27 to potentially achieve synergy in lymphocytic recruitment, including IL-18. Other potential contributing networks that could help balance the IL-6 effects included downregulation of IL-37. IL-37 co-expression along with our vectors could help reduce IL-6 effects by opposing TLR2, 4/Myd88, or p38MAPK-related pro-inflammatory signals. IL-37 is a new IL-1 family member that binds the IL-18Rα chain, suppresses innate and acquired immunity, and inhibits cytokine levels, including IL-6.[26] IL-37, IL-18, or IL-12 upregulation could help enhance IL-27 gene delivery protocols, reducing IL-6 or proinflammatory signaling to potentially enhance IL-27 effects. Other regulators upregulated in the IL-27.pepL treatment relative to IL-27.ns included IFN-γ and STAT1, and these might underlie the predicted downregulation of SOCS1.[27] Reductions in TNFAIP3, a regulator of IRF transcription might underlie the increased IFN-γ levels. The gene upregulation showed that IL-27.pepL upregulates IL-27p28 and EBI3 at higher levels than IL-27.ns, which are likely related to a feed-forward upregulation of STAT1-controlled pathways. STAT1 is a regulator of several IL-27 pathway-related promoter regions,[28] including EBI3, IL-27p28, MYC, RELA, IRF4, and IL27RA.

Comparative analyses using IPA of the IL-27 datasets (corrected to baseline pMCS) yielded several interesting canonical pathways and cellular and organismal functions that differed between the two datasets. For example, dendritic cell maturation, TREM1, and HMGB1 signaling were upregulated and LXR/RXR signaling was downregulated. TREM1 signaling could be an underlying cause of the upregulated proinflammatory cytokine genes, while HMGB1 signaling could underlie the upregulation of the immunogenic genes observed. These changes in potential immunity-related processes led us to examine the infiltration of several immune effectors *in vivo*. The tumor growth inhibition was significant in tumors

treated with pIL-27 (~50%) and further enhanced to an 89% growth inhibition in IL-27.pepL-treated tumors. This result could be due to several improvements in this therapeutic, including direct effects on the tumor cells (reductions in STAT3), as well as from indirect effects on the tumor such as a higher recruitment of effector cells including a modest but significant increase in CD3/8, a significant decrease in CD19, a normalization of CD4/25, and a significant increase in NKT cells for the IL-27.pepL-treated group relative to the mice that received IL27.ns gene delivery. Our group and others have shown that for immunogenic tumors, including those of the prostate, IL-27 can inhibit tumor growth and metastasis via increases in CD8 T cells and other effector types.[2,4,29] NKT and CD8 are potent effector lymphocytes with the capacity for killing tumor cells and recruiting other effector cell types; in particular, NKT cells serve as innate immune-regulatory cells. CD19 cell reduction could indicate a loss of B cells in tumors treated with IL-27.pepL, as well as normalization of CD4/25 levels compared to IL-27.ns, suggesting that IL-27.pepL might reverse or normalize to some extent the levels of T regulatory (Treg) cells within tumors. It is interesting that we did not detect increased NK recruitment in this tumor model. The IL-27.pepL did not seem to diminish the effect of the cytokine on γδT recruitment, and this is important as γδT cells can recognize and kill tumor cells in a tumor antigen-independent manner, potentially providing protective immune surveillance against metastatic tumors.[30] Future studies could examine the potential infiltration of other organs by effector cells, although we have not observed any significant lymphocytic infiltration.[2] However, such studies would assess the toxicity potential for this therapeutic modality. *In vivo*, we observed a significantly higher antitumor activity with the IL-27.pepL relative to IL-27.ns. One limitation of our study is that we did not examine the histopathology of the prostate tumors *in vivo* due to our main focus on the immune effectors infiltrating the tumor, and future studies will incorporate this in the design. Interestingly, when we examine expression levels of IL-27, the serum levels were highest for both therapeutics at early time points (days 7–11), but declined over time, suggesting a silencing of gene expression.

Table 1. qPCR Data Analyzed by Ingenuity Pathway Analysis

Treatment Relative to Control pMCS	Upstream Regulators Predicted Activation	Fold Change (>2.0)	Molecule Type	Upstream Regulators Predicted Inhibition	Fold Change (<−2.0)	Molecule Type
	IL-18	2.5	cytokine	MYC	−2.2	transcription regulator
	IFNG	2.4	cytokine	IRF4	−2.2	transcription regulator
	RELA	2.3	transcription regulator	NFE2L2	−2.1	transcription regulator
IL-27.ns	IRF1	2.2	transcription regulator	IL-10	−2	cytokine
	FOXO1	2.2	transcription regulator			
	TBK1	2.2	kinase			
	IL-17A	2.0	cytokine			

Treatment Relative to Control pMCS	Upstream Regulators Predicted Activation	Fold Change (>2.5)	Molecule Type	Upstream Regulators Predicted Inhibition	Fold Change (<−2.5)	Molecule Type
	IFNG	3.3	cytokine	SOCS1	−2.8	other
	IL-12	3.2	complex	BCL6	−2.6	transcription regulator
	IL-1B	3.2	cytokine	TNFAIP3	−2.6	enzyme
	TNF	3.1	cytokine	IL-37	−2.8	cytokine
	MYD88	3.1	other			
IL-27.pepL	IL-2	3.0	cytokine			
	TLR4	3.0	transmembrane receptor			
	TLR2	3.0	transmembrane receptor			
	STAT1	3.0	transcription regulator			
	IL-18	3.0	cytokine			
	P38MAPK	3.0	group			

Upstream regulators per treatment: predicted activation or inhibition and their target molecules in the dataset.
[a]p values of overlap, p < 0.001

Future studies could employ vectors with hybrid promoters such as hEF1α/HTLV or other vectors that could sustain gene expression for longer periods of time.

Additionally, studies combining wild-type or C-term targeted IL-27 with cytokines that modulate different pathways in tumor, bone, and the immune system, including some that are pro-osteogenic, are in progress. Current studies involve strategies to augment the affinity of targeting peptides beyond the micromolar levels of affinity to receptors of interest via homo- or hetero-dimerization. Future studies could explore the ability of the pepL or other related peptides to target cytokines to bone cells and/or bone matrix in vivo to further improve efficacy of IL-27.
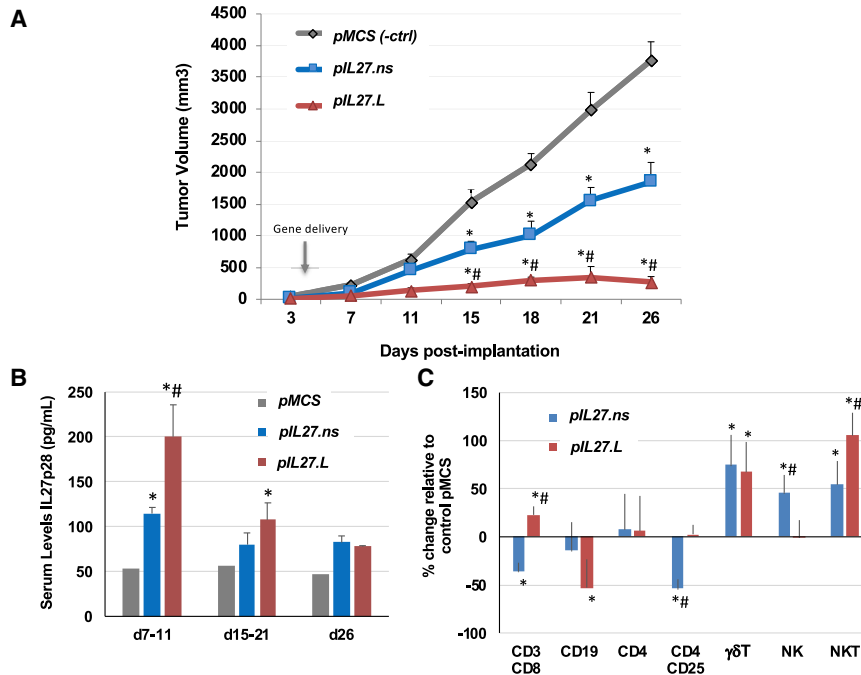
MATERIALS AND METHODS
Cell Culture
Mouse TRAMP–C2 cells were obtained from ATCC and maintained in DMEM:F12 (Mediatech, Manassas, VA) with 10% FBS and 1× Antibiotic-Antimycotic (AA, GIBCO). TRAMP-C2 cells were transduced with a lentivirus expressing activated H-ras[G12V] at a multiplicity of infection of 1 (MOI = 1) plus lentivirus transduction containing the mouse androgen receptor at MOI = 1 each to generate the TC2R line,[2] and growth comparisons between the parental TC2 and TC2R were described in Umbaugh et al.[31] RM1 cells were a gift from Dr. S. Hayward. The RM1 murine prostate cancer cell line was described in Zolochevska et al.[2] TC2R and RM1 were cultured in DMEM:F12 (Mediatech, Manassas, VA) with 10% FBS and 1× AA (GIBCO). RAW264.7 (murine monocytes) were obtained from ATCC (Manassas, VA, USA) and cultured in DMEM with 10% FBS and 1× AA (GIBCO). MC-3T3-E1 clone 14 mouse preosteoblasts were obtained from ATCC and cultured in 10% heat inactivated ATCC FBS (heat-inactivation was carried out at 55°C for 30 min followed by storage at 4°C prior to addition to media) in alpha-MEM (Invitrogen) media with 1× AA (GIBCO). HepG2, AML12, HEK293, and C2C12 were obtained from ATCC and grown in DMEM with 10% FBS and 1× AA (GIBCO). Normal prostate cells (Rwpe1 or NHpre1) were either obtained from ATCC or as a generous gift from S. Hayward and grown using a keratinocyte serum free medium kit (ATCC). PC3 were obtained from ATCC and grown in RPMI 1640 with 10% FBS and 1× AA (GIBCO). All cells except for RAW264.7 were passaged by trypsinization (0.05% [v/v] trypsin, 0.53 mM EDTA; GIBCO).

Culture Conditioned Media and Differentiation
For the Gluc binding or STAT3 reporter assays, conditioned culture media (CCM) was obtained from C2C12 muscle cells as follows: C2C12 cells were grown to 70%–80% confluence, transfected using Lipofectamine 2000 with plasmids, media changed after 6 h

A

B

C

For the paracrine versus autocrine mode of action for IL-27 experiment, using STAT1-luc assays, pepL-modified IL-27 was compared to pIL-27.ns or empty pcDNA3.1 control vector (pMCS) via assessing whether modified IL-27 signals in autocrine and paracrine modes. In the paracrine design, either differentiating osteoblast (OB, MC3T3E1-14) or TC2R epithelial cells were transfected with STAT1-luc using Lipofectamine 2000. The next day, cells were lifted, counted, and then 3×10^3 of each cell type was co-mixed with the other cell type expressing IL-27.ns, IL-27.pepL, or empty vector ctrl in 2% FBS media in 96-well white plates. In order to signal, IL-27.pepL had to be secreted from one cell type and bind to the other cell type (bearing STAT1-luc) to induce signaling. In the autocrine design, pSTAT1-luc and pIL-27 vectors were cotransfected in the same cell. An antibody used to block IL-6Rα signaling was added at cell seeding in the paracrine experiment at 0.2 μg in 100 μL (Biolegend, 115811).

For Gluc binding assays, CCM was generated as described above and utilized to treat cells seeded (10^4/well for OB, 6×10^4/well OC, and 3×10^4/well for others) in a 96-well format in a white plate (Corning), and levels of Gluc in the input were equivalent across samples (data not shown). CCM was allowed to incubate with cells at 37°C 5% CO_2 for 16 h, media removed, washed with 1× DPBS, and cells lysed in 1× Renilla lysis buffer (Promega) 40 μL. 50–100 μL Renilla substrate was added and plate was read using a Glomax luminometer (Promega) with 10 sec integration time. Results are displayed as RLU/sec.

For analyses of pepL binding to the IL-6Rα chain, we utilized the human IL-6Rα PDB 1p9m file to model the interactions. The alignment of human and mouse IL-6Rα was done using PyMol following modeling of the mouse IL-6Rα by iTASSER.[33] PepL was docked to both human and mouse IL-6Rα utilizing GalaxyPepDock,[34] which enables prediction of 3D protein-peptide complex structure

to complete DMEM/10% FBS and cells allowed to recover overnight (~16 h). The next day, cells were washed 2× in PBS, and received 2% DMEM:F12/1× AA (GIBCO) and CCM collected 48 h later. Input CCM used in the Gluc binding assay did not display significant differences in luminescence levels (data not shown). Differentiating osteoblasts (OB) were obtained by treating MC3T3E1 for 1 week with ascorbic acid and beta-glycerol phosphate from an osteogenesis kit (Millipore, ECM810) prior to Gluc cell binding assays. For differentiating RAW264.7 mouse cells into osteoclasts, cells were cultured in DMEM/10% FBS with 1× AA and gently scraped for passaging. These cells were differentiated into osteoclasts (OC) by 35 ng/mL RANKL (R&D Systems) treatment in complete media for 6 days prior to cell binding assays.

Peptide, Receptor Analysis Techniques, and Luciferase Assays

For luc reporter assays, constructs responsive to the active (phosphorylated) form of STAT1 were used (STAT1.GAS/ISRE-Luc; LR0026, Panomics, Fremont, CA) or IFN-γ-luc (Addgene, #17599) to transfect cells using Lipofectamine 2000 according to the manufacturer's protocols for each cell type and cytokine stimulation as described in.[32] For the STAT3-luc assay, C2C12 CCM was generated as described above, then CCM incubated with HEK293, PC3, RM1, or TC2R cells which had been transfected with STAT3-luc vector (Signosis, LR-2004 Panomics, Fremont, CA) using Lipofectamine 2000. Free peptides were synthesized and obtained from Selleckchem (Houston, TX). Cells were collected at 5 h or 24 h of IL-27 (or control) stimulation, lysed in passive lysis buffer (Promega, Madison, WI) and assayed in 96-well format using a Glomax luminometer with luciferin substrate (Promega).

interactions from input protein structure and peptide sequence using similar interactions found in the structure database and energy-based optimization. The modeling predicted a similar location in the IL-6Rα structure for binding of pepL, supporting the interaction with this receptor in both species.

Vectors

Plasmid DNA vectors for IL-27 expression were prepared using a pcDNA3.1 backbone. PCR cloning was utilized to clone the hyper-IL-27 cDNA from pORF9-mEBI3/p28 (Invivogen) with a 3′ insertion of a sequence encoding peptide linker (GGGGS)[35] plus the targeting peptide sequences (s7 or pepL: *LSLITRL* and as a non-specific (ns) control: *EDLGREK*, previously shown to lack any specificity for IL-6/gp130[36]). IL-27 cDNA-linker-peptide sequences were subcloned into pDrive (Promega), then excised and cloned into pcDNA3.1 using BamHI and NheI ends; empty vector control was pcDNA3.1-MCS (pMCS). Vectors were prepared for all experiments using Endofree kits (QIAGEN, Valencia, CA). For efficient complexation with polymer, vectors were first precipitated and resuspended in water. Briefly, precipitation used 1:10 volume 3M NaOAc and 2 volumes of cold 100% ethanol, followed by a 30 min incubation at −80°C and centrifugation at 12,000 rpm for 15 min at 4°C, and a wash using 2 volumes of 70% ethanol with a 5 min spin at room temp. The pellet was allowed to dry and was resuspended in sterile nuclease free water. Sonoporation of vectors intramuscularly has been described in detail previously.[13]

IPA and Real-Time PCR

For qPCR, we performed transfection of TC2R cells in a 6-well format using 5×10^5 cells and Lipofectamine 2000 according to manufacturer's protocols (Invitrogen), to introduce pcDNA3.1 empty vector (pMCS), or expressing IL-27.ns or IL-27.pepL, and collected RNA at 24 h post-transfection. The cDNA synthesis and qPCR followed procedures previously published by our group,[3] with mouse-specific primers (sequences available upon request). For network analyses, upstream regulator analysis, and downstream effect analysis, real-time qPCR data were inputted into IPA (QIAGEN Redwood City) as described in Gopurappilly and Bhonde.[37] qPCR data were generated using gene-specific primers, as described in Zolochevska et al.[3] Briefly, by comparing the imported qPCR data with the ingenuity knowledge base, a list of relevant networks, upstream regulators, and algorithmically generated mechanistic networks based on their connectivity was obtained. Only genes with a p value ≤ 0.05 were considered and both direct and indirect relationships were considered. Upstream regulator analysis was used to predict the upstream transcriptional regulators from the dataset based on the literature and compiled in the ingenuity knowledge base. The analysis examines how many known targets of the upstream regulators are present in treated cell datasets and also the direction of change as compared to control. An overlap p value is computed based on significant overlap between genes in the dataset and known targets regulated by the transcriptional regulator, with an activation Z score algorithm to make predictions. Downstream effect analysis was used to predict

activation state (increased or decreased) if the direction of change is consistent with the activation state of a biological function. Top functions (cell and organismal functions) were scored by IPA and plotted as a heatmap with p value < 2.2e-12 and sorted by predicted activation and by number of molecules, and the top 10 pathways or cellular/organismal functions were depicted. IPA calculates a B-H corrected p value for upstream regulators and for causal networks, increasing the statistical stringency of these results in core analyses.

In Vivo Studies and Intratumoral Lymphocyte Infiltration by FACS

Animal care and procedures were performed in accordance with the Purdue University institutional board guidelines (Purdue Animal Care and Use Committee or PACUC). For bioactivity assays *in vivo*, TC2R cells were transfected with luciferase reporter vectors containing either STAT1 binding sites or the IFN-γ promoter to generate "reporter cells." Equal numbers of reporter cells (7.7×10^5) were implanted in the flanks of C57BL6 males (n = 6) that had received in the hind thigh 2 days prior by sonoporation 12.5 μg of plasmid DNA (either empty control pMCS, IL-27 with a non-specific peptide [ns] at the C terminus, or C-term-targeted IL-27 [IL-27.pepL]). pDNA were delivered via sonodelivery (polymer NLSd + ultrasound + microbubbles or MB). After reporter cell injection, animals were imaged for luc activity at day 3 or day 7 post-sonoporation of pDNA. Bioluminescent signals were detectable using an IVIS100 Xenogen imager only in animals that received pIL-27.ns or pIL-27.pepL, but not pMCS control vector. For tumor implantation for IL-27 therapeutic studies, we trypsinized TC2R cells grown in in DMEM:F12 with 10% FBS and 1× AA, washed in 1× DBPS centrifugation step, then resuspended the pellet in sterile 1× DPBS and kept the cells on ice prior to implantation under isoflurane anesthesia. Male C57/BL6 mice (8–10 weeks of age) flanks were shaved and 5×10^5 TC2R cells implanted subcutaneously. Tumor growth was monitored over time using Vernier calipers to generate tumor volume measurements in mm.[3]

For gene delivery, we utilized the polymer containing a reverse nuclear localization signal (rNLS), rNLSd, a polycyclooctene with pendant tetralysine, and rNLS oligopeptide (VKRKKKP), synthesized as described in Parelkar et al.[13,38] We placed the polymers in low retention Eppendorf tubes, dissolved them in nuclease-free water, and sterilized them by filtration. The stock solution of NLSd was diluted to enable complexation with pGluc plasmid DNA at an N/P ratio of 6 (i.e., the ratio of protonatable nitrogens in the polymer, N, to DNA phosphates, P). DNA (12.5 μg) in nuclease-free water was combine with polymer in nuclease-free water at a 1:1 ratio and allowed to equilibrate for a minimum of 35 min under sterile conditions. Following polyplex formation, 5.5% sterile Micromarker microbubbles (VisualSonics, Toronto, Ontario, Canada) were added per tube and injected intramuscularly to the hind legs of male mice. After applying ultrasound gel, we sonoporated the muscle to mediate gene delivery of Gluc or IL-27 plasmids using a Sonigene instrument (VisualSonics) with 1 MHz, 20% duty cycle, and 3 W/cm^2 for 60 s.

In vivo imaging for luciferase expression in muscle was performed starting on day 4 following sonoporation using previously published procedures by intravenous luciferin substrate administration and collection of images within 15 min using an IVIS Imager with a charge-coupled device (CCD) apparatus.[39,40] For the IL-27 therapy study, we administered plasmids once intramuscularly on day 4 (tumor sizes in average of ~30 mm^3). The mice were randomized by tumor size in 3 groups relative to treatment tested, with n = 6 per group (pMCS, pIL-27.ns, pIL-27.pepL). Flow cytometry for infiltrating lymphocyte detection utilized methods and antibodies previously described.[4]

Statistical Analyses

Assays were performed in triplicate and values provided as mean ± SEM or 95% confidence interval. Comparisons were performed using unpaired t tests or one-way analysis of variance analysis using the Bonferroni t test and $p < 0.05$ considered to indicate a significant difference.

AUTHOR CONTRIBUTIONS

Conceptualization, M.L.F., T.E.; methodology, M.F.N. and M.L.F., R.L., D.C.S., R.E.D.; software, M.L.F, J.W.S., formal analysis, M.L.F., M.F.N., J.W.S.; resources, M.L.F. and T.E.; writing—original draft preparation, M.L.F and T.E.; and revisions, M.L.F., J.W.S., R.E.D., T.E.

CONFLICTS OF INTEREST

The authors declare no competing interests.

ACKNOWLEDGMENTS

REFERENCES

1. Figueiredo Neto, M., and Figueiredo, M.L. (2017). Combination of Interleukin-27 and MicroRNA for Enhancing Expression of Anti-Inflammatory and Proosteogenic Genes. Arthritis (Egypt) *2017*, 6365857.

2. Zolochevska, O., Xia, X., Williams, B.J., Ramsay, A., Li, S., and Figueiredo, M.L. (2011). Sonoporation delivery of interleukin-27 gene therapy efficiently reduces prostate tumor cell growth in vivo. Hum. Gene Ther. *22*, 1537–1550.

3. Zolochevska, O., Diaz-Quiñones, A.O., Ellis, J., and Figueiredo, M.L. (2013). Interleukin-27 expression modifies prostate cancer cell crosstalk with bone and immune cells in vitro. J. Cell. Physiol. *228*, 1127–1136.

4. Zolochevska, O., Ellis, J., Parelkar, S., Chan-Seng, D., Emrick, T., Wei, J., Patrikeev, I., Motamedi, M., and Figueiredo, M.L. (2013). Interleukin-27 gene delivery for modifying malignant interactions between prostate tumor and bone. Hum. Gene Ther. *24*, 970–981.

5. Figueiredo, M.L. (2017). Editorial: IL-27 expression following TLR activation in bone: sounding the alarm for repair. J. Leukoc. Biol. *101*, 1276–1279.

6. Dibra, D., Cutrera, J.J., Xia, X., Birkenbach, M.P., and Li, S. (2009). Expression of WSX1 in tumors sensitizes IL-27 signaling-independent natural killer cell surveillance. Cancer Res. *69*, 5505–5513.

7. Larousserie, F., Bsiri, L., Dumaine, V., Dietrich, C., Audebourg, A., Radenen-Bussière, B., Anract, P., Vacher-Lavenu, M.C., and Devergne, O. (2017). Frontline Science: Human bone cells as a source of IL-27 under inflammatory conditions: role of TLRs and cytokines. J. Leukoc. Biol. *101*, 1289–1300.

8. Yoshimoto, T., Morishima, N., Mizoguchi, I., Shimizu, M., Nagai, H., Oniki, S., Oka, M., Nishigori, C., and Mizuguchi, J. (2008). Antiproliferative activity of IL-27 on melanoma. J. Immunol. *180*, 6527–6535.

9. Pradhan, A., Lambert, Q.T., and Reuther, G.W. (2007). Transformation of hematopoietic cells and activation of JAK2-V617F by IL-27R, a component of a heterodimeric type I cytokine receptor. Proc. Natl. Acad. Sci. USA *104*, 18502–18507.

10. Lucas, S., Ghilardi, N., Li, J., and de Sauvage, F.J. (2003). IL-27 regulates IL-12 responsiveness of naive CD4+ T cells through Stat1-dependent and -independent mechanisms. Proc. Natl. Acad. Sci. USA *100*, 15047–15052.

11. Takeda, A., Hamano, S., Yamanaka, A., Hanada, T., Ishibashi, T., Mak, T.W., Yoshimura, A., and Yoshida, H. (2003). Cutting edge: role of IL-27/WSX-1 signaling for induction of T-bet through activation of STAT1 during initial Th1 commitment. J. Immunol. *170*, 4886–4890.

12. Zhu, S., Lee, D.A., and Li, S. (2010). IL-12 and IL-27 sequential gene therapy via intramuscular electroporation delivery for eliminating distal aggressive tumors. J. Immunol. *184*, 2348–2354.

13. Parelkar, S.S., Letteri, R., Chan-Seng, D., Zolochevska, O., Ellis, J., Figueiredo, M., and Emrick, T. (2014). Polymer-peptide delivery platforms: effect of oligopeptide orientation on polymer-based DNA delivery. Biomacromolecules *15*, 1328–1336.

14. Meka, R.R., Venkatesha, S.H., and Moudgil, K.D. (2018). Peptide-directed liposomal delivery improves the therapeutic index of an immunomodulatory cytokine in controlling autoimmune arthritis. J. Control. Release *286*, 279–288.

15. Su, J.L., Lai, K.P., Chen, C.A., Yang, C.Y., Chen, P.S., Chang, C.C., Chou, C.H., Hu, C.L., Kuo, M.L., Hsieh, C.Y., and Wei, L.H. (2005). A novel peptide specifically binding to interleukin-6 receptor (gp80) inhibits angiogenesis and tumor growth. Cancer Res. *65*, 4827–4835.

16. Ellis, J., Falzon, M., Emrick, T., and Figueiredo, M.L. (2014). Imaging cytokine targeting to the tumor/bone microenvironment in vivo. Hum. Gene Ther. Clin. Dev. *25*, 200–201.

17. Rousseau, F., Basset, L., Froger, J., Dinguirard, N., Chevalier, S., and Gascan, H. (2010). IL-27 structural analysis demonstrates similarities with ciliary neurotrophic factor (CNTF) and leads to the identification of antagonistic variants. Proc. Natl. Acad. Sci. USA *107*, 19420–19425.

18. Hirahara, K., Onodera, A., Villarino, A.V., Bonelli, M., Sciumè, G., Laurence, A., Sun, H.W., Brooks, S.R., Vahedi, G., Shih, H.Y., et al. (2015). Asymmetric Action of STAT Transcription Factors Drives Transcriptional Outputs and Cytokine Specificity. Immunity *42*, 877–889.

19. Ardiani, A., Farsaci, B., Rogers, C.J., Protter, A., Guo, Z., King, T.H., Apelian, D., and Hodge, J.W. (2013). Combination therapy with a second-generation androgen receptor antagonist and a metastasis vaccine improves survival in a spontaneous prostate cancer model. Clin. Cancer Res. *19*, 6205–6218.

20. Krämer, A., Green, J., Pollard, J., Jr., and Tugendreich, S. (2014). Causal analysis approaches in Ingenuity Pathway Analysis. Bioinformatics *30*, 523–530.

21. Don-Doncow, N., Marginean, F., Coleman, I., Nelson, P.S., Ehrnström, R., Krzyzanowska, A., Morrissey, C., Hellsten, R., and Bjartell, A. (2017). Expression of STAT3 in Prostate Cancer Metastases. Eur. Urol. *71*, 313–316.

22. Li, Y., Bäckesjö, C.M., Haldosén, L.A., and Lindgren, U. (2008). IL-6 receptor expression and IL-6 effects change during osteoblast differentiation. Cytokine *43*, 165–173.

23. Zhao, H., Zhang, X., Chen, X., Li, Y., Ke, Z., Tang, T., Chai, H., Guo, A.M., Chen, H., and Yang, J. (2014). Isoliquiritigenin, a flavonoid from licorice, blocks M2 macrophage polarization in colitis-associated tumorigenesis through downregulating PGE2 and IL-6. Toxicol. Appl. Pharmacol. *279*, 311–321.

24. Natividad, K.D., Junankar, S.R., Mohd Redzwan, N., Nair, R., Wirasinha, R.C., King, C., Brink, R., Swarbrick, A., and Batten, M. (2013). Interleukin-27 signaling promotes immunity against endogenously arising murine tumors. PLoS ONE *8*, e57469.

25. Wei, J., Xia, S., Sun, H., Zhang, S., Wang, J., Zhao, H., Wu, X., Chen, X., Hao, J., Zhou, X., et al. (2013). Critical role of dendritic cell-derived IL-27 in antitumor immunity through regulating the recruitment and activation of NK and NKT cells. J. Immunol. *191*, 500–508.

26. Conti, P., Ronconi, G., Kritas, S.K., Caraffa, A., and Theoharides, T.C. (2018). Activated Mast Cells Mediate Low-Grade Inflammation in Type 2 Diabetes: Interleukin-37 Could Be Beneficial. Can. J. Diabetes 42, 568–573.

27. Sandling, J.K., Garnier, S., Sigurdsson, S., Wang, C., Nordmark, G., Gunnarsson, I., Svenungsson, E., Padyukov, L., Sturfelt, G., Jönsen, A., et al. (2011). A candidate gene study of the type I interferon pathway implicates IKBKE and IL8 as risk loci for SLE. Eur. J. Hum. Genet. 19, 479–484.

28. Rouillard, A.D., Gundersen, G.W., Fernandez, N.F., Wang, Z., Monteiro, C.D., McDermott, M.G., and Ma'ayan, A. (2016). The harmonizome: a collection of processed datasets gathered to serve and mine knowledge about genes and proteins. Database (Oxford) 2016, 2016.

29. Murugaiyan, G., and Saha, B. (2013). IL-27 in tumor immunity and immunotherapy. Trends Mol. Med. 19, 108–116.

30. Dieli, F., Vermijlen, D., Fulfaro, F., Caccamo, N., Meraviglia, S., Cicero, G., Roberts, A., Buccheri, S., D'Asaro, M., Gebbia, N., et al. (2007). Targeting human gammadelta T cells with zoledronate and interleukin-2 for immunotherapy of hormone-refractory prostate cancer. Cancer Res. 67, 7450–7457.

31. Umbaugh, C.S., Diaz-Quiñones, A., Neto, M.F., Shearer, J.J., and Figueiredo, M.L. (2017). A dock derived compound against laminin receptor (37 LR) exhibits anti-cancer properties in a prostate cancer cell line model. Oncotarget 9, 5958–5978.

32. Bluyssen, H.A., and Levy, D.E. (1997). Stat2 is a transcriptional activator that requires sequence-specific contacts provided by stat1 and p48 for stable interaction with DNA. J. Biol. Chem. 272, 4600–4605.

33. Roy, A., Kucukural, A., and Zhang, Y. (2010). I-TASSER: a unified platform for automated protein structure and function prediction. Nat. Protoc. 5, 725–738.

34. Lee, H., Heo, L., Lee, M.S., and Seok, C. (2015). GalaxyPepDock: a protein-peptide docking tool based on interaction similarity and energy optimization. Nucleic Acids Res. 43 (W1), W431-5.

35. Sockolosky, J.T., Kivimäe, S., and Szoka, F.C. (2014). Fusion of a short peptide that binds immunoglobulin G to a recombinant protein substantially increases its plasma half-life in mice. PLoS ONE 9, e102566.

36. Manfredini, R., Tenedini, E., Siena, M., Tagliafico, E., Montanari, M., Grande, A., Zanocco-Marani, T., Poligani, C., Zini, R., Gemelli, C., et al. (2003). Development of an IL-6 antagonist peptide that induces apoptosis in 7TD1 cells. Peptides 24, 1207–1220.

37. Gopurappilly, R., and Bhonde, R. (2015). Transcriptional profiling and functional network analyses of islet-like clusters (ILCs) generated from pancreatic stem cells in vitro. Genomics 105, 211–219.

38. Parelkar, S.S., Chan-Seng, D., and Emrick, T. (2011). Reconfiguring polylysine architectures for controlling polyplex binding and non-viral transfection. Biomaterials 32, 2432–2444.

39. Zolochevska, O., and Figueiredo, M.L. (2009). Expression of cell cycle regulator cdk2ap1 suppresses tumor cell phenotype by non-cell-autonomous mechanisms. Oral Oncol. 45, e106–e112.

40. Zolochevska, O., Yu, G., Gimble, J.M., and Figueiredo, M.L. (2012). Pigment epithelial-derived factor and melanoma differentiation associated gene-7 cytokine gene therapies delivered by adipose-derived stromal/mesenchymal stem cells are effective in reducing prostate cancer cell growth. Stem Cells Dev. 21, 1112–1123.